Radiation of sound into a cylindrical enclosure from a point-driven end plate with general boundary conditions

Li Cheng[a)] and Jean Nicolas
G.A.U.S., Mechanical Engineering Department, Université de Sherbrooke, Sherbrooke, Québec J1K 2R1, Canada

(Received 8 March 1991; accepted for publication 21 November 1991)

The radiation of sound from a point-driven circular plate into a hard-walled cylindrical enclosure is investigated. Emphasis is given on studying the effects of the boundary conditions of the plate, which are modeled as a continuous distribution of edge springs acting against both the deflection and the rotation of the contour of the plate. With this model, both classical and intermediate boundary cases can be simulated by adjusting the elastic stiffness of the springs. A coupled acoustoelastic formulation is developed following a variational approach, with the use of hard-walled cavity modes. In the analysis, the full interaction between the structure vibration and the internal cavity sound pressure is considered. Numerical results indicate that a significant reduction in noise inside the cavity can be obtained for a relatively wide frequency range by completely relaxing the translational support (zero deflection stiffness) of the plate. This is mainly due to a weakening of the modal radiation efficiency of the flexural modes of the plate. With an increase of the deflection stiffness on the contour of the plate, this beneficial frequency range is shifted to higher frequencies. It is hoped that the findings of the present work will be useful for practical predictions of airplane cabin noise emitted by the rear pressure bulkhead, as well as for noise control in some aerospace structures and mechanical systems involving cylindrical-shaped cavities.

PACS numbers: 43.50.Lj, 43.40.Rj, 43.20.Tb

INTRODUCTION

The radiation of sound by vibrating structures into an acoustical enclosure has received a great deal of attention in the past 30 years. The problem is of considerable importance in many engineering applications, especially in the field of aerospace or automobile engineering, where the externally excited vibrating walls of vehicles induce a significant internal sound field. In architectural acoustics, where a rectangular room is usually involved, the minimizing of the internal noise level radiated by wall partitions is also one of the major applications.

The problem is rather complex in nature because of the structure–cavity coupling. In order to reveal the fundamental phenomena of the problem, scientists chose systems having a relatively simple geometry, among which the following configuration is often used: a rectangular plate backed by a rectangular cavity. This model was first investigated by Lyon[1] in 1963. In his work, the noise reduction for such a cavity-backed plate was investigated in a straightforward but approximate manner, since with a small cavity many assumptions were made regarding the plate–cavity coupling. Then, Dowell and Voss[2] studied the effect of the cavity on the natural frequencies of the plate. This phenomenon was confirmed by further investigations of Pretlove.[3,4] Moreover, he showed that the effects of shallow cavities on the vibration of a plate are not negligible.

The problem was then investigated in more detail by many researchers such as Bhattacharya and Crocker,[5] Guy,[6,7] McDonald *et al.*,[8] and Vaicaitis.[9] A general formulation of the structure–cavity interaction problem was given by Dowell *et al.*[10] in 1977. Extensive work based upon Dowell's formulation followed: For example, Narayanan[11,12] considered the sound transmission properties of sandwich panels. The work of Cheng *et al.*[13] presented some theoretical and experimental results on the damping effects of the panel–cavity system. Pan *et al.*[14,15] presented another analysis on a similar subject.

This literature review shows that a large amount of work has been done, yet very little is known about the effect of the boundary conditions of the plate on the radiated sound field. In fact, most of the papers mentioned above dealt with simply supported plates. Only a few studies[8,13] treated clamped plates, and the most detailed information available is that given by Narayanan *et al.*,[12] who used a plate with two simply supported edges. Therefore, there is a lack of general formulation and understanding of the effects of boundary conditions. One of the most plausible reasons for this may be that these studies rely heavily on the knowledge of the in-vacuum normal modes of the plates, and the latter is known analytically only for some very special boundary condition cases. Many questions, however, concerning structural boundary conditions are of great importance, and have to be answered: What are the effects of the classical boundary conditions of a cavity-backed structure (free, freely guided, simply supported, and clamped); what are the consequences of elastic support; finally, what are the guidelines to be followed for improving the structure-induced sound field inside the cavity?

[a)] Present address: Mechanical Engineering Department, Université Laval, Québec G1K 7P4, Canada.

In this paper we present an attempt to answer these questions with a point-driven circular plate exciting an enclosed cylindrical sound field. The choice of this configuration comes mainly from a practical motivation. In fact, the work reported in this paper is one step of a long-term research activity focusing on the cabin noise of airplanes powered by turbofan jet engines. Two main components enclosing the cabin are the fuselage skin and a circular rear pressure bulkhead (RPB), to which the engines are attached through a beamlike structure. Preliminary testings on the plane revealed that mechanical excitation was one of the main noise sources. Therefore the RPB, which is a circular platelike structure, may be a strong sound radiator. As a preliminary model, the plane cabin is considered as a cylindrical cavity having an acoustically rigid wall (with infinite impedance). A thorough understanding of the effects of the boundary conditions of the RPB can, hopefully, help the engineer reduce the cavity noise. The work reported here does not purport to offer a general model for airplane cabin noise predictions. Instead, rather powerful procedures have already been established, such as the one reported by Pope.[16] The interests of the present work are twofold: First, with regards to airplane cabin noise, to investigate the effects of the RPB, an element that has not received sufficient attention up to now in the literature; second, to extend the existing knowledge regarding the boundary conditions of a plate in the general plate–cavity coupling problem.

The model used for this study is a circular plate backed by a circular cylindrical cavity. The plate is driven by an external point force and is elastically supported by rotational and translational springs along its edge. With this model, both classical boundary conditions and intermediate cases can be easily simulated by making use of different combinations of the elastic constants of the springs. A variational formulation associated with a Rayleigh–Ritz approach is used in the analysis of the plate by choosing simple polynomials as trial functions. The same method has been used by the authors for a free vibration analysis of a plate–shell system.[17] The reader is referred to this work for more details about the plate vibration. For the cavity, the hard-walled cavity modes are used as a basis for the decomposition of the sound pressure and also for obtaining the Green's function of the cavity. The resulting coupling equations, in which the full interactions between the structure vibration and the internal cavity pressure field are taken into account, are then solved.

The proposed formulation for the vibration of the plate is shown to be an interesting alternative to the classical modal decomposition approaches used by most researchers in the problem of plate–cavity coupling. In fact, our formulation encompasses all the boundary condition cases in a general way, removing all previous restrictions in this regard. Thanks to a better understanding of the phenomena, this may offer practitioners new possibilities for the challenge of noise control.

This paper is organized as follows: In Sec. I we outline the main procedure and results of the analytical formulation, ending with several comments on numerical implementation. In Sec. II, numerical results are presented and discussed. First, the effects of some classical boundary conditions of the plate are considered. Then, the modal radiation behavior of the plate is investigated to give an interpretation of the phenomena observed. Finally, the study on elastically supported cases reveals the possibilities and limitations of soundproofing by changing the structural boundary conditions. The conclusions are then presented in Sec. III.

I. THEORETICAL DEVELOPMENT

A. Description of the model

The theoretical model considered is a plate–cavity system, as shown in Fig. 1. The cavity (of radius a and length l) is a circular cylinder with one wall (A_F) at $z=0$ being a circular flexible plate (of thickness h_p), while all the other walls (A_R), including the end of the cylinder at $Z=1$, are acoustically rigid. The plate is elastically supported by translational and rotational springs uniformly distributed around its edge Γ. The translation along the plate edge is therefore supported by translational springs having a distributed stiffness K (N/mm) and the rotation is supported by rotational springs having a distributed stiffness C (N). The plate is assumed to be thin and only flexural vibrations are taken into account. A point force $F(t)$ in the positive z-axis direction is applied to the plate at the point (r_F,θ_F). In what follows, the sound field within the cavity, as well as the vibration of the plate, will be calculated. The fluid loading on the plate from outside the cavity will be neglected.

B. Vibrations of the plate

As part of a structure already studied, the free vibration of the plate has been described in a previous work,[17] and the reader is referred to this work for more details. Here special attention is paid only to the excitation terms by which the plate is coupled to the cavity.

The equation of motion of the structure is obtained by finding the extremum of Hamilton's function H for the structure over a suitable subspace of displacement trial functions. For the circular plate considered in Sec. I A, Hamilton's function H can be expressed as follows:

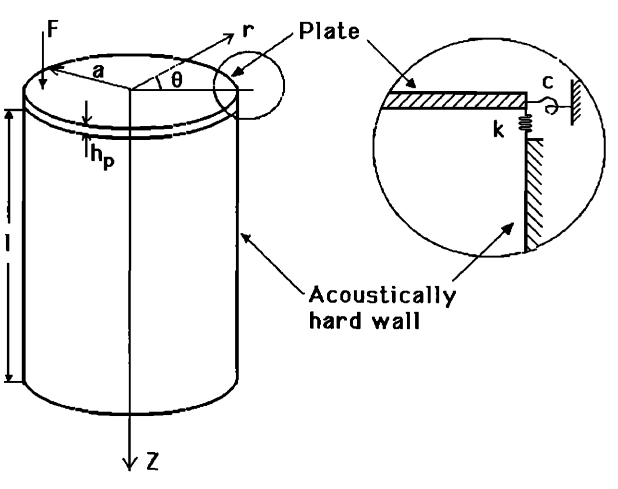

FIG. 1. Geometry of the problem and coordinate systems employed in the formulation.

$$H=\int_{t_0}^{t_1}(T_P-E_P-E_K+E_F)dt, \quad (1)$$

where t_0 and t_1 are arbitrary times, T_p and E_p are, respectively, the kinetic energy and the potential energy of the plate, E_K is the elastic energy stored in the springs, E_F is the work done by the driving point force $F(t)$ and by the internal sound pressure $P_c(t)$. The first three terms are given in Appendix A, and E_F is written as

$$E_F=\int_0^a\int_0^{2\pi}[P_c(t)\cdot w_p(t)-F(t)\delta(r-r_F) \times\delta(\theta-\theta_F)w_p(t)]r\,d\theta\,dr, \quad (2)$$

where $w_p(t)$ is the flexural displacement of the plate, $P_c(t)$ is the sound pressure inside the cavity, and δ denotes the Dirac distribution.

The plate displacement $w_p(t)$ is then expanded over a set of suitable trial functions. For an elastically supported plate, no geometric conditions are imposed *a priori* and a simple polynomial decomposition is chosen as follows:

$$w_p(t)=\sum_{\alpha=0}^{1}\sum_{n=0}^{\infty}\sum_{m_p=0}^{\infty}B^{\alpha}_{nm_p}(t)\Lambda^{\alpha}_{nm_p},$$
$$\Lambda^{\alpha}_{nm_p}=\sin(n\theta+\alpha\cdot\pi/2)(r/a)^{m_p}, \quad (3)$$

with n, m_p, and α being, respectively, the circumferential order, the radial order, and the symmetry index. The $B^{\alpha}_{nm_p}(t)$ are coefficients to be determined.

In the case where sinusoidal motion is assumed,

$$F(t)=F\exp(j\omega t);\quad P_c(t)=P_c\exp(j\omega t);$$
$$w_p(t)=w_p\exp(j\omega t);\quad B^{\alpha}_{nm_p}(t)=B^{\alpha}_{nm_p}\exp(j\omega t), \quad (4)$$

where ω is the excitation angular frequency.

Inserting Eqs. (3) into (1) gives Hamilton's function H in terms of the unknown coefficients $B^{\alpha}_{nm_p}(t)$. Obtaining the extremum of H with respect to the $B^{\alpha}_{nm_p}(t)$ yields the equation of movement of the plate. Using expression (4), one has

$$\sum_{m_p'=0}^{\infty}(R^{\alpha}_{nm_pm_p'}(1+j\eta_p)-\omega^2M^{\alpha}_{nm_pm_p'})B^{\alpha}_{nm_p'} +\sum_{m_p'=0}^{\infty}aN^{(1)}_{\alpha n}\left[K+\left(\frac{m_p}{a}\right)\left(\frac{m_p'}{a}\right)C\right]B^{\alpha}_{nm_p'} =F^{\alpha}_{nm_p}-P^{\alpha}_{nm_p}, \quad (5)$$

where m_p' is the current value of the index m_p. The expressions for the stiffness term $R^{\alpha}_{nm_pm_p'}$, the mass term $M^{\alpha}_{nm_pm_p'}$ and the function $N^{(1)}_{\alpha n}$ have been given in Appendix B. The excitation terms $F^{\alpha}_{nm_p}$ and $P^{\alpha}_{nm_p}$ are

$$F^{\alpha}_{nm_p}=\int_{A_F}F\delta(r-r_F)\delta(\theta-\theta_F)\Lambda^{\alpha}_{nm_p}\,dA_F,$$
$$P^{\alpha}_{nm_p}=\int_{A_F}P_c\Lambda^{\alpha}_{nm_p}\,dA_F. \quad (6)$$

In Eq. (5), a structural damping model has been introduced by means of a complex Young's modulus, and η_p is the associated loss factor. It can be seen that the plate is coupled to the acoustic cavity via the last term of the right-hand side of Eq. (5).

C. Sound field within the cavity

The sound pressure inside the cavity is treated here in a rather classical way. The pressure, as well as Green's function for the cavity, are expanded in terms of the normal modes of the acoustically rigid-walled cavity. The orthogonality of these modes enables us to reduce the problem to a set of ordinary differential equations with structural coupling terms.

The acoustic pressure P_c inside the cavity is governed by the classical wave equation

$$\nabla^2P_c+(\omega/c)^2P_c=0, \quad (7)$$

where c is the speed of sound.

The continuity of velocities on the different parts of the cavity walls is expressed by

$$\frac{\partial P_c}{\partial\bar n}=\rho\omega^2w_p,\quad \text{on } A_F,$$
$$\frac{\partial P_c}{\partial\bar n}=0,\quad \text{on } A_R, \quad (8)$$

where ρ is the fluid density, A_F and A_R are, respectively, the flexible and rigid portion of the cavity wall surface, and $\bar n$ is the unit normal to the corresponding surface (positive toward the outside).

It has been shown[18] that the sound pressure P_c inside the cavity can be calculated by means of Green's function G with the Neumann boundary condition,

$$P_c=-\int_A G\frac{\partial P_c}{\partial\bar n}dA;\quad A=A_FUA_R. \quad (9)$$

Using Eq. (8), the above expression becomes

$$P_c=-\int_{A_F}G\rho\omega^2w_p\,dA_F. \quad (10)$$

The Green's function in the cavity, which satisfies the Neumann boundary condition, can be calculated if the cavity modes are known:[18]

$$G(M_v,M_v',\omega)=\sum_{N=1}^{\infty}\frac{c^2}{VM_N}\frac{\phi_N(M_v)\phi_N(M_v')}{(\omega_N^2-\omega^2)}, \quad (11)$$

$$\frac{1}{V}\int_v\phi_N(M_v)\phi_M(M_v)dv=M_N\delta_{NM}, \quad (12)$$

where $\phi_N(M_v)$ and ω_N are, respectively, the nth cavity normal mode shape and angular frequency, V is the volume occupied by the cavity, and M_v, M_v' are two arbitrary points in the cavity. Here δ_{NM} is the Kronecker delta.

The pressure inside the cavity can then be expanded in terms of the cavity modes as

$$P_c=\rho c^2\sum_{N=1}^{\infty}\frac{P_N\phi_N}{M_N}, \quad (13)$$

in which the P_N are the pressure coefficients to be determined. Substituting Eqs. (11)–(13) into Eq. (10) gives

$$(\omega_N^2-\omega^2)P_N=(A_F/V)\omega^2w_N, \quad (14)$$

$$w_N = \frac{1}{A_F}\int_{A_F} w_p \cdot \phi_N \, dA_F. \quad (15)$$

For the acoustically hard-walled cylindrical cavity considered here, the normal modes are analytically known. In this case, the nth mode is represented by the four indices α, n, p, q, and the cavity mode shape and the corresponding angular frequency are calculated by

$$\phi^{\alpha}_{npq} = \sin[n\theta + \alpha(\pi/2)] J_n(\lambda_{np} r)\cos[(q\pi/1)z], \quad (16)$$

$$\omega^{\alpha}_{npq} = c[\lambda^2_{np} + (q\pi/1)^2]^{1/2}, \quad (17)$$

where α is the symmetry index, n is the circumferential order, J_n is the nth-order Bessel function, q is the longitudinal order, and λ_{np} is the pth root of the following equation:

$$J'_n(\lambda_{np} a) = 0. \quad (18)$$

By using Eq. (12), the modal generalized mass M^{α}_{npq} can also be calculated.

Considering the displacement decomposition of the plate [Eq. (3)], together with Eqs. (15) and (16), Eq. (14) becomes

$$(\omega^2_{npq} - \omega^2) P^{\alpha}_{npq} = -\omega^2\left(\frac{A_F}{V}\right)\sum_{m_p=0}^{\infty} L(\alpha,n,p,m_p) B^{\alpha}_{nm_p}, \quad (19)$$

where $L(\alpha,n,p,m_p)$ is the spatial coupling coefficient between the plate and the cavity:

$$L(\alpha,n,p,m_p) = \frac{1}{A_F}\int_{A_F} \Lambda^{\alpha}_{nm_p}\phi^{\alpha}_{npq} \, dA_F. \quad (20)$$

The damping in the cavity can be expressed in terms of a modal damping factor η_v. Consequently, Eq. (19) can be written as

$$(\omega^2_{npq} + j\eta_v \omega_{npq}\omega - \omega^2) P^{\alpha}_{npq} = -\omega^2\left(\frac{A_F}{V}\right)\sum_{m_p=0}^{\infty} L(\alpha,n,p,m_p) B^{\alpha}_{nm_p}. \quad (21)$$

D. Structure–cavity coupling equations

The pressure term appearing at the right-hand side of Eq. (5) can now be expressed by substituting Eqs. (3) and (13) into the second expression of Eqs. (6), giving

$$P^{\alpha}_{nm_p} = \rho c^2 A_F \sum_{p=1}^{\infty}\sum_{q=0}^{\infty} L(\alpha,n,p,m_p)\frac{P^{\alpha}_{npq}}{M^{\alpha}_{npq}}. \quad (22)$$

Substituting Eq. (22) into Eq. (5) while taking into account Eq. (21) yields the structure–cavity coupling equations:

$$\sum_{m'_p=0}^{\infty}\left[R^{\alpha}_{nm_pm'_p}(1+j\eta_p) - \omega^2 M^{\alpha}_{nm_pm'_p}) B^{\alpha}_{nm'_p}\right] + \sum_{m'_p=0}^{\infty} aN^{(1)}_{\alpha n}\left[K + \left(\frac{m_p}{a}\right)\left(\frac{m'_p}{a}\right)C\right]B^{\alpha}_{nm'_p} = F^{\alpha}_{nm_p} - \rho c^2 A_F \sum_{p=1}^{\infty}\sum_{q=0}^{\infty} L(\alpha,n,p,m_p)\frac{P^{\alpha}_{npq}}{M^{\alpha}_{npq}}, \quad (23)$$

$$(\omega^2_{npq} + j\eta_v \omega_{npq}\omega - \omega^2) P^{\alpha}_{npq} = -\omega^2\left(\frac{A_F}{V}\right)\sum_{m_p=0}^{\infty} L(\alpha,n,p,m_p) B^{\alpha}_{nm_p}. \quad (24)$$

It can be seen from Eq. (24) that the cavity unknowns P^{α}_{npq} can be expressed in terms of the $B^{\alpha}_{nm_p}$. Therefore, the two sets of equations can be combined by eliminating the P^{α}_{npq}. Consequently, (23) becomes

$$\sum_{m'_p=0}^{\infty}\left[R^{\alpha}_{nm_pm'_p}(1+j\eta_p) - \omega^2 M^{\alpha}_{nm_pm'_p}) B^{\alpha}_{nm'_p}\right] + \sum_{m'_p=0}^{\infty} aN^{(1)}_{\alpha n}\left[K + \left(\frac{m_p}{a}\right)\left(\frac{m'_p}{a}\right)C\right]B^{\alpha}_{nm'_p} = F^{\alpha}_{nm_p} - \sum_{m'_p=0}^{\infty}\sum_{p=1}^{\infty}\sum_{q=0}^{\infty} Z^{\alpha}_{npqm_pm'_p} B^{\alpha}_{nm'_p}, \quad (25)$$

with

$$Z^{\alpha}_{npqm_pm'_p} = \frac{\rho c^2 A^2_F \omega^2 L(\alpha,n,p,m_p)\cdot L(\alpha,n,p,m'_p)}{V\cdot(\omega^2_{npq} + j\eta_V \omega_{npq}\omega - \omega^2) M^{\alpha}_{npq}}. \quad (26)$$

The most particular feature of the coupling equations (25) is the selective manner in which the structural response can only couple spatially with a limited number of acoustic modes. In fact, the structural terms having a circumferential order n and a symmetry index α excite only acoustic modes that have the same circumferential order and symmetry index.

E. Comments

1. Solution of the equations and definition of characteristic parameters

Two types of problems can be solved by using the established model: free vibrational analysis of a plate in vacuum and structure–cavity coupling analysis.

The free vibrational study of a plate can be made by neglecting the right-hand terms of Eq. (25). The solution of this eigenvalue equation yields the natural frequencies together with the coefficients for constructing the mode shapes. A set of results has been reported by the authors for a circular plate with general boundary conditions.[17] Comparisons with some previously reported results showed excellent agreement.

The structure–cavity coupling analysis, which is the main topic of the present work, can be achieved by solving Eq. (25). The acoustic sound field can then be determined by Eqs. (24) and (13). Two main parameters will be used in the analysis.

(i) the average quadratic velocity of the plate $\langle V^2\rangle$,

$$\langle V^2\rangle = \frac{\omega^2}{2A_F}\int_{A_F} w_p w^*_p \, dA_F. \quad (27)$$

In the following, $\langle V^2\rangle$ is presented in dB referenced to $2.5\times 10^{-15}\ \mathrm{m^2/s^2}$:

(ii) the average sound pressure level inside the cavity L_p,

$$L_p = 10\log(\langle P^2_c\rangle/p^2_0), \quad p_0 = 2\times 10^{-5} p,$$

$$\langle P^2_c\rangle = \frac{1}{2V}\int P_c P^*_c \, dV. \quad (28)$$

2. Simulation of the boundary conditions

The boundary conditions of the plate have been previously modeled to be elastic. The limiting cases such as simply supported, clamped, freely guided, or free plates can be obtained by setting the appropriate constant K or C equal to either zero or infinity. For infinity, one considers a sufficiently large value in the numerical calculations. For this, we define nondimensional stiffness parameters with respect to the flexural rigidity of the plate D_p as follows:

$$\overline{K} = Ka^3/D_p, \quad \overline{C} = Ca/D_p.$$

In numerical results that will be presented later, the infinite value of $\overline{K}$ or $\overline{C}$ is produced by taking a value of 10^8 in each case.

3. Truncation of the linear equations

For computation purposes, the dimension of the linear system (23) and (24) has to be truncated to a finite order. For the plate, this has been done by taking 15 terms for n and 13 terms for m_p in the expansion series Eq. (3). For the configuration used in this work, this is found to be sufficient to cover the frequency range of interest $(0 - f_{\max})$ up to 2000 Hz. As far as the cavity is concerned, all cavity modes whose natural frequencies are included in the frequency range of interest have been taken in the expansion (13). For certain values of n where the natural frequency of even the lowest cavity mode is higher than $f_{\max}$, the first nine lowest modes have been taken into consideration.

II. NUMERICAL RESULTS AND DISCUSSION

The numerical results that are presented here are for a steel plate having a 0.25-m radius and a thickness of 0.003 m, whose critical frequency is about 4000 Hz. A cylindrical cavity of the same radius and having a depth of 0.6 m is filled with air. The plate is driven by a unit point force at $r_F = 0.1$ m and $\theta_F = 0$. The loss factors of the plate and the cavity are assumed to be constant: $\eta_v = \eta_p = 0.01$.

Numerical results and comments are presented in following order: First, taking a free plate as an example, a brief description regarding the fluid–structure coupling is given in terms of system modes. Second, plates with classical boundary conditions are analyzed. The so-called classical boundary conditions are defined as the following: free case ($K = 0$, $C = 0$); guided case ($K = 0$, $C = \infty$); simply supported case ($K = \infty$, $C = 0$); and clamped case ($K = \infty$, $C = \infty$). Note that these are four typical cases resulting from the different combinations of the limiting values of the edge stiffnesses K (translational) and C (rotational). Although free supports, as well as guided supports, can hardly be justified in practical circumstances for cavity configurations, they do act as very informative reference cases for understanding phenomena. In addition, as will be illustrated later, with the decreasing of the stiffness of the supports, the phenomena observed in the free case become rather representative of more realistic cases. Third, the radiation behavior of a single plate mode is investigated with the aim of producing a comprehensive understanding of the problem. Finally, plates with intermediate elastic supports are considered, as this case is useful for more practical cases.

A. Modal coupling between the plate and cavity

In the theory formulated above, the plate–cavity coupled system is described in terms of the natural modes of its two uncoupled subsystems; the *in vacuo* plate and the acoustically hard-walled cavity. Generally speaking, when the plate and the cavity are coupled together, these modes are affected by the coupling. This problem has been investigated by some authors,[2,3,19] who used simply supported and clamped plates to show that the normal modes of the coupled system can be divided into two groups: plate-controlled modes and cavity-controlled modes, the distinction depending on whether the modes are dominated by plate vibrations or the cavity sound field. It is generally admitted that with a light fluid (such as air), this coupling effect is weak for deep cavities.[2] Based on some assumptions regarding the nature of the coupling at low frequencies, both plate-controlled modes and cavity-controlled modes can be rather accurately estimated by some simple formulas.[19]

Before proceeding to the effects of the boundary conditions, we observe the spectrum of the sound pressure level induced by a free plate to show this coupling phenomenon (Fig. 2). The peaks emerging in the curve are marked by different symbols. Those marked by a square represent plate-controlled modes, corresponding basically to the resonances of the *in vacuo* plate with a slight shift due to the coupling with the cavity. The peaks marked by a circle are cavity-controlled modes. For these two types of modes, the uncoupled natural modes of the two subsystems form a good approximation of the actual modes at low frequencies, where the modal density is low (less than 0.5% for the present case). However, it should be stressed that this observation cannot be generalized, since the nature of the coupling between the plate and the cavity depends greatly on the characteristics of the system. As an example, a shallow cavity may increase the frequency of fundamental plate resonance by as much as 15%.[2] Therefore, consideration of the full coupling is recommended if precise information is required. In Fig. 2, the first peak indicated by a triangle is characteristic of free

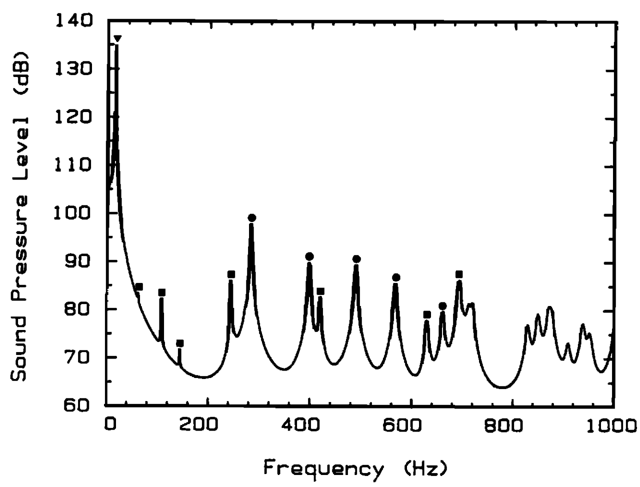

FIG. 2. Overall sound pressure level inside the cavity radiated by a free plate. ■: plate-controlled modes; ●: cavity-controlled modes; ▼: pumping mode.

(or guided) plates, corresponding to the piston motion of the plates supported by the aerostatic stiffness of the cavity. This special mode will be shown to produce a strong cavity sound field at its resonant frequency. Let us term it the "pumping frequency" f_p and proceed to estimate it.

Upon assuming that only the rigid cavity mode (with a zero natural frequency) affects the system, the frequency for the fundamental mode of the plate f_{coupled} (modified by coupling with the cavity) can be approximated by[19]

$$f_{\text{coupled}} = \left(\frac{1}{2\pi}\right)\left(f_{\text{in vacuo}} + \frac{\rho c^2 A_F^2 L_{0s}^2}{(M_S V)}\right)^{1/2}, \tag{29}$$

where M_S is the generalized modal mass of the plate and L_{0s} is the coupling coefficient between a plate mode and a cavity mode, defined as the integral of their mode shapes over the contacting surface:

$$L_{0s} = \frac{1}{A_F}\int_{A_F} \phi_0 \Pi_s \, dA_F, \tag{30}$$

with ϕ_0 and Π_s being, respectively, the mode shapes of the rigid cavity mode and the fundamental mode of the plate *in vacuo*.

For the present case of a free circular plate, the fundamental plate mode is a piston motion. Thus $f_{in\ vacuo} = 0$, $\Pi_s = 1$, $M_s = \rho_p h_p A_F$, ρ_p and h_p being, respectively, the density and thickness of the plate. For the rigid cavity mode, $\phi_0 = 1$. Using these relations, Eq. (29) becomes

$$f_{\text{coupled}} = f_p = (1/2\pi)\sqrt{\rho c^2/(\rho_p h_p l)}. \tag{31}$$

Therefore, the three main parameters determining the "pumping frequency" of a free plate are the rigidity of the acoustic medium ρc^2 (having units of N/m^2), the surface density of the plate $\rho_s h_p$, and the cavity depth l.

Expression (31) can also be written in a different form:

$$f_p = (1/2\pi)\sqrt{K_p/(\rho_p h_p A_F)},$$
$$K_p = \rho c^2 A_F / l. \tag{32}$$

It can be seen that K_p is the aerostatic stiffness of the cylindrical cavity. In the present configuration $K_p = 4.54 \times 10^4$ N/m. Hence, the "pumping frequency" of the system can be simply and precisely calculated by this formula.

B. Plates with classical boundary conditions

As far as the effect of the boundary conditions of the plate, Fig. 3(a)–(c) shows the results for plates with simple supports (solid lines) and free supports (dashed lines). Figure 3(a) shows the comparison in terms of the average quadratic velocity of the plate $\langle V^2 \rangle$. The difference between the two curves is caused mainly by the different positions of the plate-controlled resonances. Generally speaking, the overall level of the plate vibration is not affected much by the boundary conditions of the plates. Figure 3(b) compares the corresponding average sound pressure level within the cavity L_p, as defined by Eq. (28). In addition to the plate-controlled resonances, already perceived in the quadratic velocity spectra, one can also notice the peaks corresponding to the cavity-controlled resonances. Except at very low frequencies, the free plate radiates much less than a simply supported

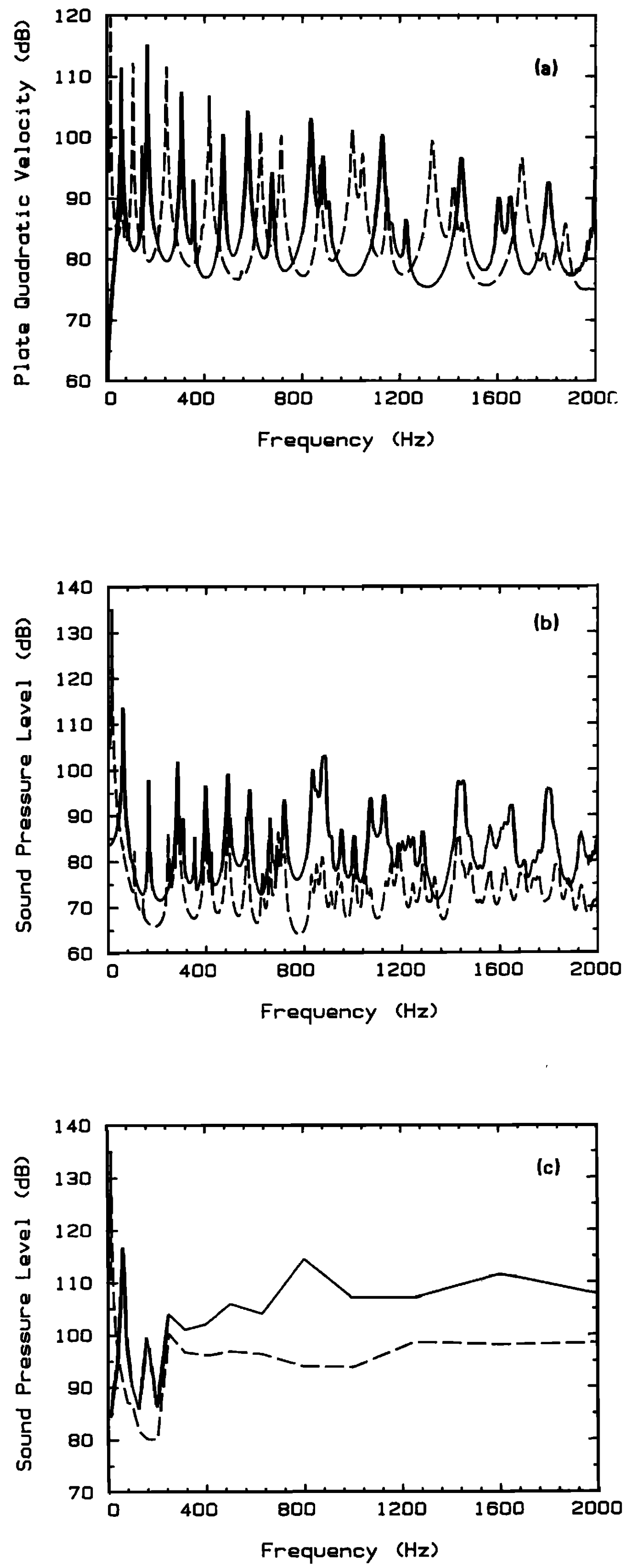

FIG. 3. Overall sound pressure level inside the cavity and average velocity of the plates with two different boundary conditions: simply supported (solid lines) and free (dashed lines). (a) Average quadratic velocity of the plates in narrow bands. (b) Overall sound pressure level inside the cavity in narrow bands. (c) Overall sound pressure level inside the cavity in one-third octave bands.

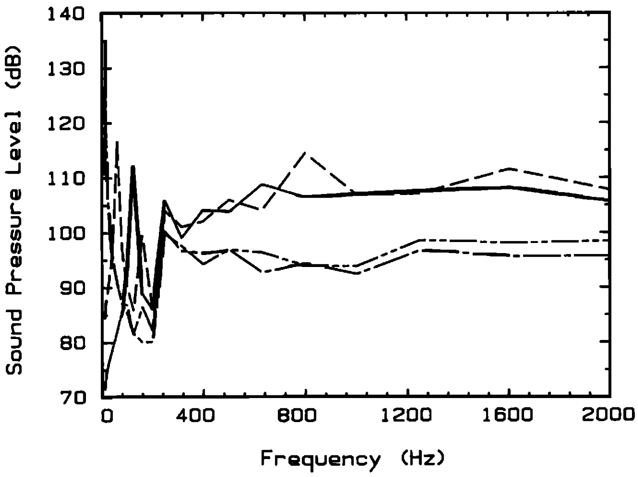

FIG. 4. Overall sound pressure level inside the cavity (in one-third octave bands) radiated by plates with different boundary conditions: Clamped (solid lines); simply supported (dashed lines); guided (dot–dashed lines); and free (double dot–dashed lines).

one. This can be more clearly seen in Fig. 3(c), in which the sound pressure is shown for one-third octave bands. One observes that the sound pressure level induced by a free plate is 10–20 dB lower than the one radiated by a simply supported plate. This is true for almost the entire frequency range from 50–2000 Hz in the present case. The exception occurs in the low-frequency range centered at 16 Hz, where the free plate gives a stronger sound field than a simply supported one. This is the pumping mode of the plate analyzed in the previous section. The fact that this mode contributes significantly to the cavity sound field and that the cavity produces non-negligible stiffness shows that the mode is well coupled.

Figure 4 shows the sound pressure level L_p radiated from plates with the four classical boundary conditions: clamped supports, simple supports, guided supports, and free supports. The results are presented using one-third octave bands. Although the comparisons are not very apparent at low frequencies (below 200 Hz), where the plate modal density is low and the sound field may be completely controlled by particular plate modes, one notices roughly the same radiation capacity for the clamped and simply supported plates on the one hand, and for the guided and free plates on the other. Therefore, it can be concluded that the translational stiffness of the contour supports, K, is a key factor in the radiation behavior of the plates into the cavity. It seems that a lightly deflected support will reduce the sound level inside the cavity. This issue will be addressed in Sec. II D, where the case of elastic supports is examined.

C. Modal radiation behavior of cylindrical cavity-backed plates

As representative examples, a free plate and a simply supported plate are used to reveal the radiation mechanism of plates with different boundary conditions.

As is known, one of the most useful parameters in far-field radiation problems is the radiation efficiency, defined as the ratio of the radiated power to a quantity proportional to the quadratic velocity of the structure. However, for the cavity problem, as pointed out by one of the present authors,[19] this parameter is no longer suitable, mainly because of the standing wave properties of the cavity. In fact, in this case the radiated power as defined in the classical way becomes the power absorbed by dissipation factors of the cavity such as damping and absorption. As a result, from the point of view of physics and physiology, it is no longer a parameter as relevant as acoustic energy or sound pressure. To this end, we use another parameter $\bar{\sigma}$ that we call the "Radiation Efficiency into Cavity" (REC), and it is defined as the ratio of the acoustic energy in the cavity E_{VA} to the kinetic energy of the plate E_{pl}:

$$\bar{\sigma} = 10\ \text{Log}(E_{VA}/E_{\text{pl}}),$$
$$E_{VA} = \frac{1}{2}\int_V \frac{|P_c|^2}{\rho c^2}\,dv,$$
$$E_{\text{pl}} = \frac{1}{2}\rho_p h_p A_F \langle V^2 \rangle. \qquad (33)$$

It is worth noting that $\bar{\sigma}$ is a nondimensional factor and applies not only to the whole structure, but also to a single mode of the structure. In the latter case, the arguments in-

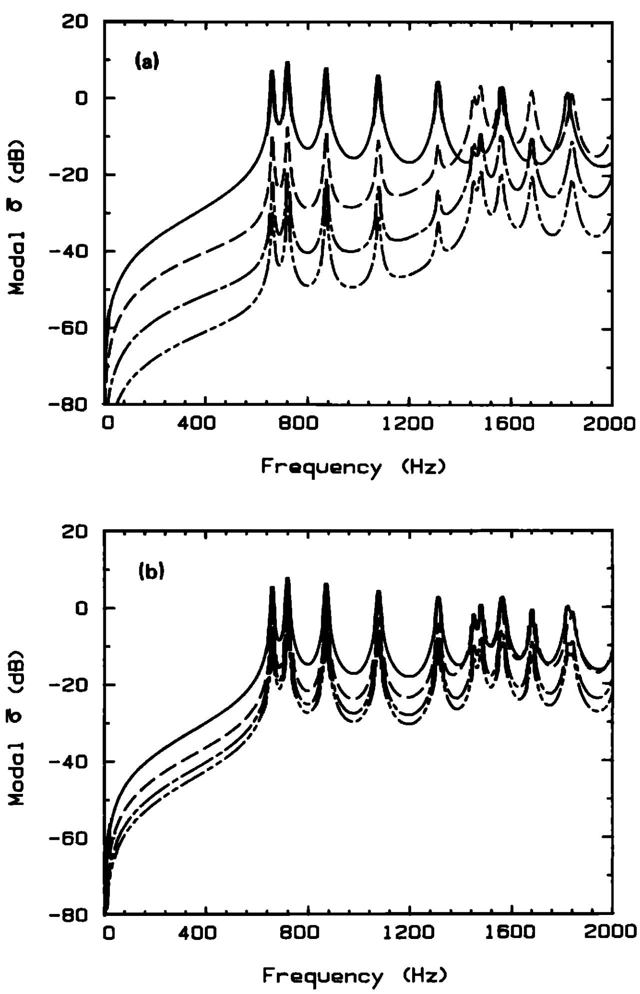

FIG. 5. The $\bar{\sigma}$ (REC) for various modes of the plates: Mode (2,1) (solid lines); mode (2,2) (dashed lines); mode (2,3) (dot–dashed lines); mode (2,4) (double dot–dashed lines). (a) Free plate; (b) Simply supported plate.

volved in the above definition will be those induced by the structural mode in question. In order to avoid any misunderstanding, it should be stressed that the term "radiation efficiency" used in this paper refers to the $\bar{\sigma}$ defined above. Since the acoustic energy is involved in the definition, it will not be surprising to see the modal properties of the cavity from this parameter.

Figure 5 shows the radiation characteristics of several modes of the plate, for the cases of free supports [Fig. 5(a)] and simple supports [Fig. 5(b)]. The four modes illustrated are (2,1), (2,2), (2,3), and (2,4). For the identification of a plate mode, a pair of numbers is used, where the first number denotes the circumferential order while the second identifies the mode rank by increasing value of the natural frequencies. It can be observed that, in both cases, $\bar{\sigma}$ is weighted by the cavity resonances of the same circumferential order (two for the present case). One important feature that should be noted is that the $\bar{\sigma}$ of the lower-order modes are generally higher than those of the higher-order ones.

A comparison between these two cases allows one to understand the weak radiation of the free plates. For the same series of modes, this comparison is presented in Fig. 6(a)–(d) by drawing separately the $\bar{\sigma}$ of the free plate modes together with the equivalent for the case of the simply supported plate. The diagrams are arranged in an increasing order of modes. Figure 6(a) shows that the (2,1) mode exhibits roughly the same radiation capacity for both types of boundary conditions. As for the (2,2) mode [Fig. 6(b)], there is a visible difference between these two curves, indicating that the free plate mode radiates less. As the mode order increases this tendency becomes more and more apparent, as is seen in the successive figures. For the (2,4) mode, which is the highest of the four modes considered, Fig. 6(d) shows a difference of some 15–20 dB. Numerical studies show that this observation applies to a varying degree to the other plate modes as well.

This observation is consistent with the one made previously for the far-field sound radiation from baffled plates. In that case, as was pointed out by Skudrzyk[21] and Williams,[22] the low radiation efficiency of the free plate modes is the result of the cancellation occurring between adjacent cells. In a recent work on rectangular plates, Berry *et al.*[23] showed that the piston motion alone is sufficient to provide a good estimate for the radiated power from a free plate, and that the piston motion is in turn a poor radiator. In the present analysis, it has been observed that this predominant role

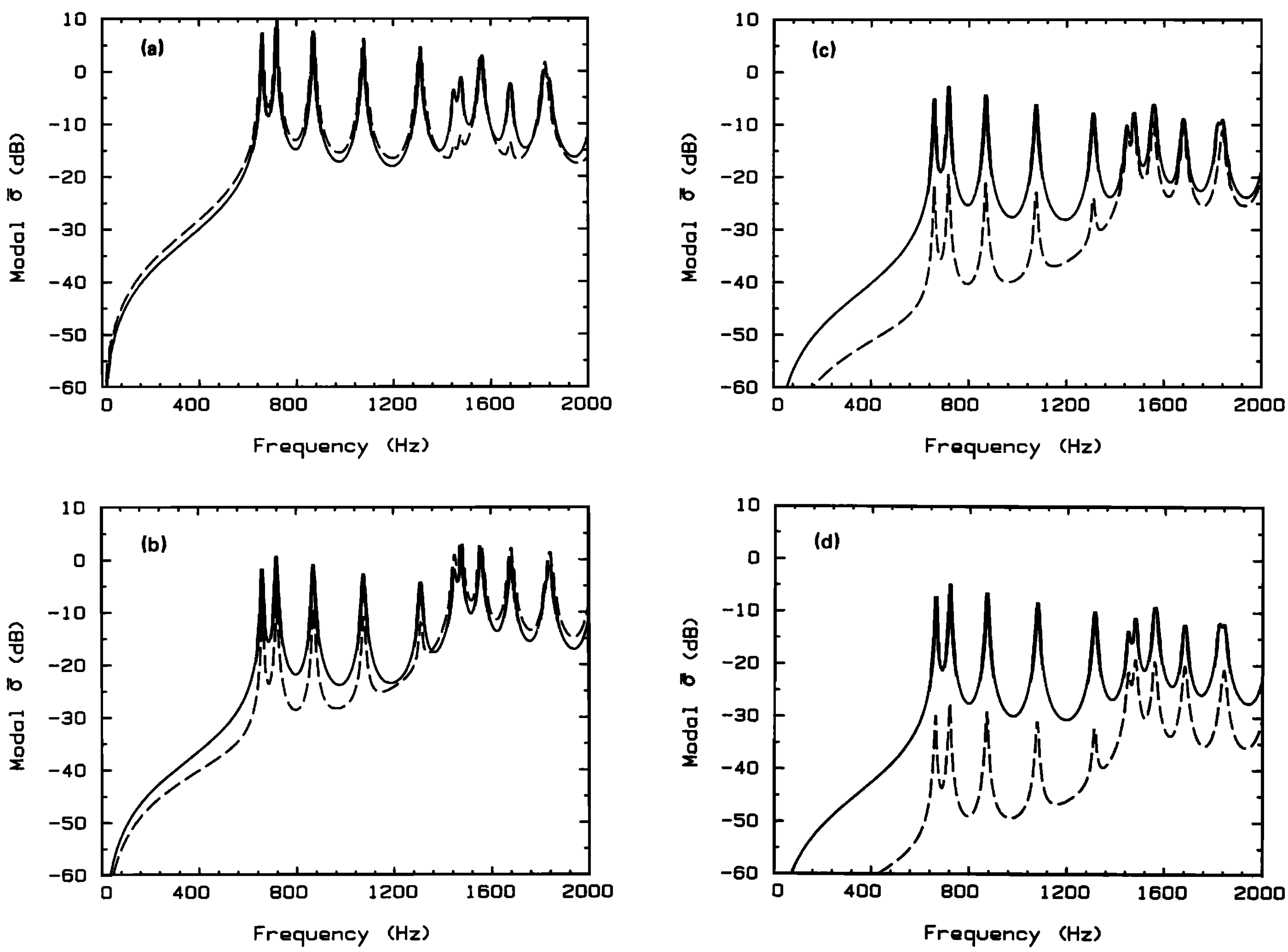

FIG. 6. The $\bar{\sigma}$ (REC) for various modes of a simply supported plate (solid lines) and of a free plate (dashed lines). (a) Mode (2,1); (b) mode (2,2); (c) mode (2,3); (d) mode (2,4).

of the piston motion for free field radiation is no longer true for cavity problems. This is mainly because the flexural modes, which may generate evanescent waves in the far-field radiation case, become significant contributors to the sound field within an enclosure. Therefore, in our case, the low radiation capacity of the flexural modes of the free plate becomes the primary factor. It is believed that such information would be useful at the design stage of such systems.

D. Plates with intermediate elastic supports

The two previous sections have focused on some idealized and limiting boundary condition cases. The fact that a free plate or a guided plate radiates much less than a simply supported plate or a clamped plate for a relatively wide frequency range may be beneficial in engineering applications. In other words, this suggests relaxing the deflection restraints at the plate contour to improve the sound field in the cavity. Realistically, however, completely free cases do not exist, the structures having to be supported in some manner. Therefore, it seems necessary to consider elastic support cases to reveal their practical possibilities and limitations. Here, we can take advantage of the generality of our formulation to get closer to practical situations.

Figure 7 compares a simply supported plate with three elastically supported plates in terms of the sound pressure level L_p calculated in one-third octave bands. For the three elastic cases, the plates are supported only by translational springs, the stiffness of which are, respectively, $10K_p$, $100K_p$, and $1000K_p$, where K_p is the aerostatic stiffness of the cylindrical cavity, as defined by expression (32). To give an approximate estimate of the rigidity of the supports, the natural frequency corresponding to the piston motion for the three cases are, respectively, 52.4, 158.8, and 499.9 Hz.

Two main conclusions can be drawn from these results. First, in comparison to the free cases, a limiting frequency seems to exist for each elastic support, above which the plate behaves roughly like a free plate. (For the sake of clarity, the curve corresponding to the free plate has been purposely omitted.) In fact, the response of the plate supported by $10K_p$ can be shown to be nearly the same as that of the free plate from the one-third octave band centered at 200 Hz. For the two other elastically supported cases, this limiting frequency is, respectively, 800 and 2000 Hz. This frequency can be more accurately determined from the spectra in narrow bands. Second, a comparison with the simply supported plate, represented by the solid line in Fig. 7, illustrates how elastic supports affect the cavity sound pressure. The analysis of Sec. II B outlined the weak radiating property of the free plate. Therefore, the fact that elastically supported plates behave nearly like a free one above their respective limiting frequencies indicates a significant reduction in induced sound pressure, as is clearly shown in Fig. 7. Indeed, this beneficial effect begins to occur even slightly before this limiting frequency. However, in the frequency range below this value, a softer support does not always guarantee a reduction in sound. The reason is that different supporting conditions modify the structural modes, the consequence of which can further change the modal structural–cavity coupling. As a result, in some frequency ranges, the cavity sound

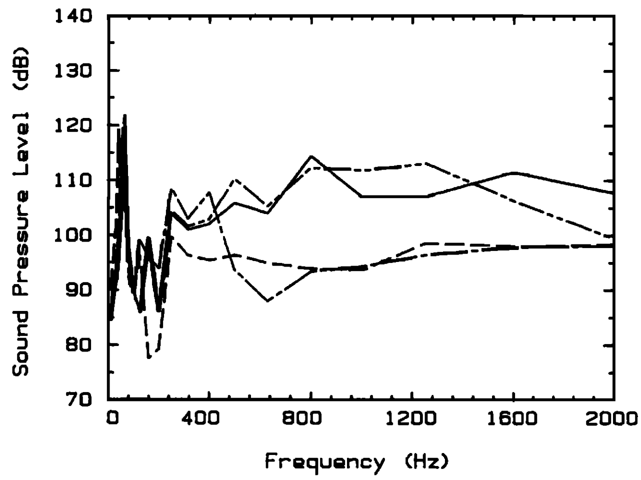

FIG. 7. Overall sound pressure level inside the cavity (in one-third-octave bands) radiated by plates with simply supported or elastic supports against deflection. Simply supported plate: Solid line. The stiffness of the elastic supports are, respectively, $10K_p$ (dashed lines); $100K_p$ (dot–dashed lines); $1000K_p$ (double dot–dashed lines), where K_p is defined by Eq. (32).

pressure may be amplified. Combining these two observations, one concludes that the stiffer the support is, the higher is this limiting frequency and, consequently, the higher up is the frequency range where the beneficial effect is expected.

III. CONCLUSIONS

The radiation of sound from a point-driven circular plate into a closed cylindrical enclosure has been investigated. The study was motivated by the desire to obtain an understanding of the noise emitted by the rear pressure bulkhead into the cabin of an airplane. In a larger context, this work aimed to deepen the existing understanding regarding the effects of the boundary conditions of plates and to offer new possibilities for noise control. The simulation of the boundary conditions of the plates is made possible by means of elastic support modeling. The elastic constants for the contour of the plate are chosen to simulate free, guided, simply supported, and clamped edges as well as other intermediate cases. In the formulation, the full coupling between the sound pressure field inside the cavity and the structural motion is taken into account. The sound field generated outside the cavity is neglected in the analysis. For a typical configuration, numerical results are presented and the phenomena observed are interpreted.

It is shown that the deflection stiffness on the contour of the plate plays an important part in determining the radiated sound field within the cavity. For a very wide frequency range, a significant reduction can be obtained by reducing the rigidity of the deflection supports of the plate, the exception being at low frequencies where the response may be controlled by particular plate modes. As limiting cases, a free or a guided plate is shown to radiate much less sound into the cavity than a simply supported or clamped one in a frequency range above a so-called "pumping frequency" f_p of the former. This is mainly because of the low radiation capacity of the flexural modes of the free or guided plate. In situations where the plate is elastically supported against deflection, it seems that a limiting frequency exists above which the plate behaves roughly like a free plate, and consequently where a beneficial effect in the sound level is expected, but below which a negative effect may occur because of the particular modal coupling. This limiting frequency is shown to increase with the deflection stiffness of the supports. This analysis illustrates that an improvement in the internal sound field is possible by the choice of a suitably low deflection stiffness for the structure.

This paper has focused on a numerical study of the problem. Although some measurements confirming partial findings of the present work have been done, more effort is still needed to carry out complete experimental investigations. Moreover, further analysis seems to be necessary to address the case of nonrigid cavity walls. This will need the simulation of a system comprising the entire plate–shell structure coupled to the acoustic enclosure. These issues should be addressed by subsequent research.

ACKNOWLEDGMENT

The authors thank John Quaroni of the National Research Council of Canada for doing the revision in English of this paper.

APPENDIX A: ENERGY EXPRESSIONS OF THE PLATE

Here we have

$$T_p = \frac{1}{2}\rho_p h_p \int_0^{2\pi}\int_0^a \left(\frac{\partial w_p}{\partial t}\right)^2 r\, d\theta\, dr, \qquad \text{(A1)}$$

$$E_p = \frac{D_p}{2}\int_0^{2\pi}\int_0^a \Bigg\{\left(\frac{\partial^2 w_p}{\partial r^2} + \frac{1}{r}\frac{\partial w_p}{\partial r} + \frac{1}{r^2}\frac{\partial^2 w_p}{\partial \theta^2}\right)^2 - 2(1-\nu_p)\left[\frac{\partial^2 w_p}{\partial r^2}\left(\frac{1}{r}\frac{\partial w_p}{\partial r} + \frac{1}{r^2}\frac{\partial^2 w_p}{\partial \theta^2}\right)\right] + 2(1-\nu_p)\left[\frac{\partial}{\partial r}\left(\frac{1}{r}\frac{\partial w_p}{\partial \theta}\right)\right]^2\Bigg\} r\, d\theta\, dr, \qquad \text{(A2)}$$

$$E_k = \frac{1}{2}\int_0^{2\pi}\left\{\left[K w_p^2 + C\left(\frac{\partial w_p}{\partial r}\right)^2\right]_{r=a} a\, d\theta\right\}, \qquad \text{(A3)}$$

where ρ_p and h_p are, respectively, the density and the thickness of the plate; $D_p = E_p h_p^3/12(1-\nu_p^2)$ represents the flexural rigidity of the plate, with ν_p and E_p being, respectively, the Poisson's ratio, and the Young's modulus of the shell material. In the above expressions, w_p should be read as $w_p(t)$ as used in Eq. (2), meaning that w_p is time dependent.

APPENDIX B: EXPRESSIONS OF $R^{\alpha}_{nm_pm'_p}$, $M^{\alpha}_{nm_pm'_p}$, AND $N^{(1)}_{\alpha n}$

$$R^{\alpha}_{nm_pm'_p} = \frac{D_p \Psi_{m_pm'_p}}{a^2}\{N^{(1)}_{\alpha n}[(m_p^2-n^2)(m_p'^2-n^2) - (1-\nu_p)m_p(m_p-1)(m'_p-n^2) - (1-\nu_p)m'_p(m'_p-1)(m_p^2-n^2)] + 2(1-\nu_p)N^{(2)}_{\alpha n}n^2(m_p-1)(m'_p-1)\}, \qquad \text{(B1)}$$

$$M^{\alpha}_{nm_pm'_p} = a^2\rho_p h_p N^{(1)}_{\alpha n}/(m_p+m'_p+2), \qquad \text{(B2)}$$

$$N^{(1)}_{\alpha n} = \begin{cases}\pi, & \text{for } n\neq 0,\\ 0, & \text{for } n=0 \text{ and } \alpha=0,\\ 2\pi, & \text{for } n=0 \text{ and } \alpha=1,\end{cases} \qquad \text{(B3)}$$

where

$$\Psi_{m_pm'_p} = \begin{cases}0, & \text{for } m_p+m'_p-2\leqslant 0,\\ 1/(m_p+m'_p-2), & \text{otherwise;}\end{cases} \qquad \text{(B4)}$$

$$N^{(2)}_{\alpha n} = \begin{cases}\pi, & \text{for } n\neq 0,\\ 0, & \text{for } n=0 \text{ and } \alpha=1,\\ 2\pi, & \text{for } n=0 \text{ and } \alpha=0.\end{cases} \qquad \text{(B5)}$$

[1] R. H. Lyon, "Noise reduction of rectangular enclosures with one flexible wall," J. Acoust. Soc. Am 35, 1791–1799 (1963).

[2] E. H. Dowell and H. M. Voss, "The effect of a cavity on panel vibration," AIAA 1, 476–477 (1963).

[3] A. J. Pretlove, "Free vibration of a rectangular panel backed by a rectangular cavity," J. Sound. Vib. 2, 197–209 (1965).

[4] A. J. Pretlove, "Forced vibration of a rectangular panel backed by a closed rectangular cavity," J. Sound Vib. 3, 252–261 (1966).

[5] M. C. Bhattacharya and M. J. Crocker, "Forced vibration of a panel and radiation of sound into a room," Acustica 22, 275–294 (1969/70).

[6] R. W. Guy and M. C. Bhattacharya, "The transmission of sound through a cavity-backed finite plate," J. Sound Vib. 27, 207–223 (1973).

[7] R. W. Guy, "The response of a cavity-backed panel to external airborne excitation: A general analysis," J. Acoust. Soc. Am. 65, 719–731 (1979).

[8] B. W. McDonald, R. Vaicaitis, and M. K. Myers, "Noise transmission through plates into an enclosure," NASA No. TP-1173, 1987.

[9] R. Vaicaitis, "Noise transmission by viscoelastic sandwich panels," NASA TN D-8516, 1977, p. 40.

[10] E. H. Dowell, G. F. Gorman, and D. A. Smith, "Acoustoelasticity: General theory, acoustic natural modes, and forced response to sinusoidal excitation, including comparison with experiment," J. Sound Vib. 52, 519–542 (1977).

[11] S. Yarayanan and R. L. Shanbhag, "Acoustoelasticity of a clamped sandwich panel backed by a cavity," J. Sound Vib. 74, 453–473 (1981).

[12] S. Yarayanan and R. L. Shanbhag, "Sound transmission through elastically supported sandwich panels into a rectangular enclosure," J. Sound Vib. 77, 251–270 (1981).

[13] L. Cheng and C. Lesueur, "Influence des amortissements sur la réponse vibroacoustique, Étude théorique et expérimentale d'une plaque excitée mécaniquement et couplée avec une cavité," J. Acoust. 2, 347–355 (1989).

[14] J. Pan and D. A. Bies, "The effect of fluid-structural coupling on sound waves in an enclosure—Theoretical part," J. Acoust. Soc. Am. 87, 691–707 (1990).

[15] J. Pan and D. A. Bies, "The effect of fluid–structural coupling on sound waves in an enclosure—Experimental part," J. Acoust. Soc. Am 87, 708–717 (1990).

[16] L. D. Pope, "On the prediction of propeller tone sound levels and gradients in an airplane cabin," J. Acoust. Soc. Am. 88, 2755–2765 (1990).

[17] L. Cheng and J. Nicolas, "Free vibration analysis of a cylindrical shell-circular plate system with general coupling and various boundary conditions," J. Sound Vib. 154 (2), (1992).

[18] P. M. Morse and K. U. Ingard, *Theoretical Acoustics* (McGraw-Hill, New York, 1968), Chap. 9, pp. 467–607.

[19] L. Cheng, "Etude vibroacoustique d'une structure couplée à une cavité: Étude des effets de dissipation—recherche de lois de similitude," Ph.D. thesis, 89-ISAL0042, INSA-Lyon, France, 1989, pp. 45–52.

[20] P. Millot, "Rayonnement acoustique de plaques couplées dans une cavité," Ph.D. Thesis, 87-ISAL0033, INSA-Lyon, France, 1987.

[21] E. Skudrzyk, *Simple and Complex Vibratory Systems* (The Pennsylvania State University Press, University Park, PA, 1968).

[22] E. G. Williams, "A series expansion of the acoustic power radiated from planar sources," J. Acoust. Soc. Am. 73, 1520–1524 (1983).

[23] A. Berry, J.-L. Guyader, and J. Nicolas, "A general formulation for the sound radiation from rectangular, baffled plates with arbitrary boundary conditions," J. Acoust. Soc. Am. 88, 2792–2802 (1990).